Compound-Nucleus Decay along the Mass-Asymmetry Coordinate and the Role of the Businaro-Gallone Point

L. G. Sobotka,[a] M. A. McMahan, R. J. McDonald, C. Signarbieux,[b] G. J. Wozniak, M. L. Padgett, J. H. Gu,[c] Z. H. Liu,[d] Z. Q. Yao,[c] and L. G. Moretto

Nuclear Science Division, Lawrence Berkeley Laboratory, University of California, Berkeley, California 94720

(Received 23 July 1984)

Fragments with atomic numbers covering the entire range of the mass-asymmetry coordinate ($Z=1$ to $Z=Z_{CN}/2$) were observed from the decay of compound nuclei (CN) produced in reactions of 7.4- and 8.4-MeV/nucleon ^{74}Ge, ^{93}Nb, and ^{139}La with ^{9}Be and ^{12}C. The evolution of the charge distribution with increasing mass of the compound nucleus ($A=83$ to 151) reflects the topological change in the potential-energy surface associated with crossing the Businaro-Gallone point.

PACS numbers: 25.70.Gh, 25.70.Jj, 25.85.Ge

The sharp distinction between evaporation and fission in relatively heavy compound nuclei is a result of a specific topological feature of the liquid-drop-model potential-energy surface $V(Z)$ as a function of mass asymmetry Z. This feature is a deep minimum at symmetry (fission region) flanked at greater asymmetries by the Businaro-Gallone mountains which in turn descend at even larger asymmetries ("evaporation" region). The corresponding mass distribution from compound-nucleus (CN) decay is approximately proportional to $\exp[-V(Z)/T_Z]$ and shows a peak at symmetry (fission peak) and two wings at the extreme asymmetries (evaporation wings). The qualitative dependence of the potential energy and of the mass yield versus asymmetry is shown in Fig. 1(a) for a heavy nucleus.

With decreasing total mass the potential energy surface undergoes a topological change when the fissility parameter x crosses the so-called Businaro-Gallone point.[1] At this point ($x_{BG}=0.396$ for $l=0$ and decreases for larger l values) the second derivative of the potential energy with respect to the mass-asymmetry coordinate evaluated at symmetry vanishes.[1-3] Thus below the Businaro-Gallone point there is no longer a traditional fission saddle point, and the monotonically increasing potential energy towards symmetry implies the disappearance of fission as a process distinct from evaporation. Thus the mass distribution should show the two evaporation wings extending as far as symmetry where a minimum should be observed. This is illustrated in Fig. 1(b).

Such a transition has never been observed, as it requires the measurement of the entire mass distribution from symmetry to the extreme asymmetry of α,p evaporation for a series of systems straddling the Businaro-Gallone point. This measurement is made very difficult by the low yield for symmetric decay of the compound nucleus in this general mass region, and by the need to verify that the products were produced by a compound-nucleus mechanism.[4]

In this Letter we communicate the measurement of complete charge distributions from protons to symmetric splitting as well as the successful verification of the Businaro-Gallone transition. Such a transition is inferred from the disappearance of the

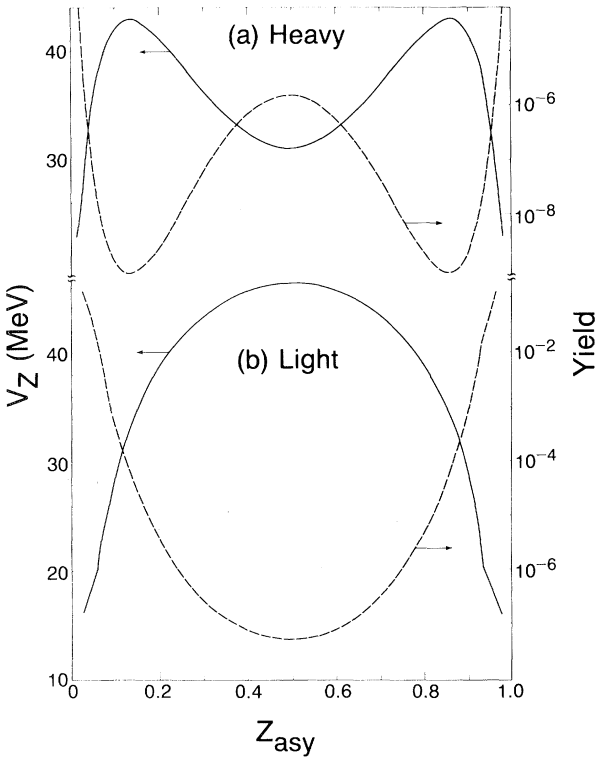

FIG. 1. Comparison of the potential energy surfaces (solid curve) and expected yields (dashed curve) for (a) a heavy CN (Au at $l=0$ and $E^*=97$ MeV) and (b) a light CN (Ge at $l=0$ and $E^*=72$ MeV).

TABLE I. The excitation energies, angular momenta, fissility x, and rotational y parameters for compound nuclei produced in the reactions Ge,Nb, La + Be.

CN	E^* (MeV)	l_{max} ($\hbar$)	l_{crit} ($\hbar$)	x [a]	y_m [b]
^{83}Kr	73.2	36	35	0.31	0.008
^{102}Rh	77.3	42	39	0.40	0.06
^{148}Eu	70.4	42	46	0.50	0.03

[a] $x = Z^2/50A$. [b] $y = 2l_m^2/A^{7/3}$.

fission peak in the mass yield as the compound-nucleus mass was decreased from ^{148}Eu to ^{102}Rh to ^{83}Kr. The excitation energies, angular momenta, fissility x, and rotational y parameters for the compound nuclei studied are listed in Table I.

The use of reverse kinematics (projectile heavier than the target) was crucial in performing these measurements. This technique virtually eliminates the problems associated with low-cross-section measurements due to the presence of light-element target contaminants. Furthermore, reverse kinematics provides a large center-of-mass (c.m.) velocity which facilitates the verification of full momentum transfer and allows easy identification of the fragment's atomic number at the higher laboratory energies. Finally the high-energy solution at forward angles corresponds to very backward angles in ordinary kinematics. This should enhance the observation of compound-nucleus decay and virtually eliminate any possible deep-inelastic contamination.

The experiments were carried out at the Lawrence Berkeley Laboratory SuperHILAC utilizing beams of 550-MeV ^{74}Ge, 782-MeV ^{93}Nb, and 1157-MeV ^{139}La, to bombard targets of 0.54 mg/cm^2 ^{12}C and 1.0 mg/cm^2 ^{9}Be. The detection system consisted of four solid state ΔE-E silicon telescopes (40–70 μm, 3–5 mm) situated at 7.5°, 15°, 25°, and 35° from the beam with solid angles of approximately 1.0 msr. For the heavier ^{139}La beam these detectors were supplemented by two gas ΔE–solid-state-E telescopes at −7.5° and −22.5°.

The observed laboratory energies represent only the higher-energy kinematic solution. In general, the lower solution is not observed because of the energy threshold due to the thickness of our ΔE detectors. Thus the laboratory energy of the upper solution, the measured atomic number (Z), and angle permitted us to verify that the recorded events both originated from a system with full momentum transfer and had a c.m. energy independent of angle. This is shown for two representative

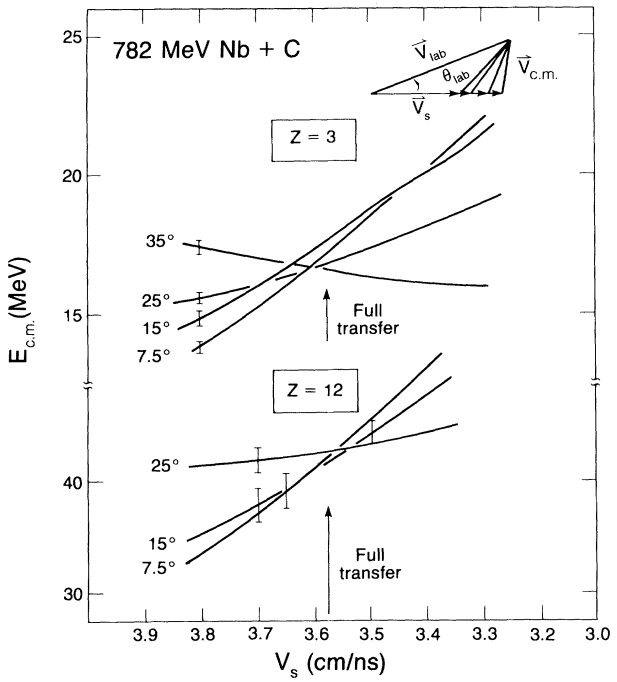

FIG. 2. The line for each angle gives the locus of solutions for both $E_{c.m.}$ and V_s. The intersection of the various lines fixes these quantities. The velocity corresponding to complete linear momentum transfer is indicated. This figure was drawn with the assumption that the masses follow the line of β stability.

elements in Fig. 2.

The mean laboratory energies for each Z value were converted to velocities with two different assumptions for the relationship between the Z and the mass of the detected fragments. These velocities are then decomposed into two components. One component, along the beam direction, is assigned an arbitrary value; the other component is that required to reconstitute the original velocity. (For convenience this second component is shown as the c.m. energy in Fig. 2.) In this way, for each laboratory angle we can draw a curve representing the dependence of the c.m. energy upon the source velocity. This procedure is followed for each angle that is smaller than the kinematically allowed maximum angle. The intersection of these lines determines, in a model-independent way, both the momentum transfer and the energy in the center of mass. The error bars shown on the lines in Fig. 2 reflect the uncertainty in the mean laboratory energies.

The results from this type of analysis for the ^{93}Nb + ^{12}C system are shown in Fig. 3. The upper part of this figure demonstrates that with either mass assumption all of the measured products result from the decay of a system with full momen-

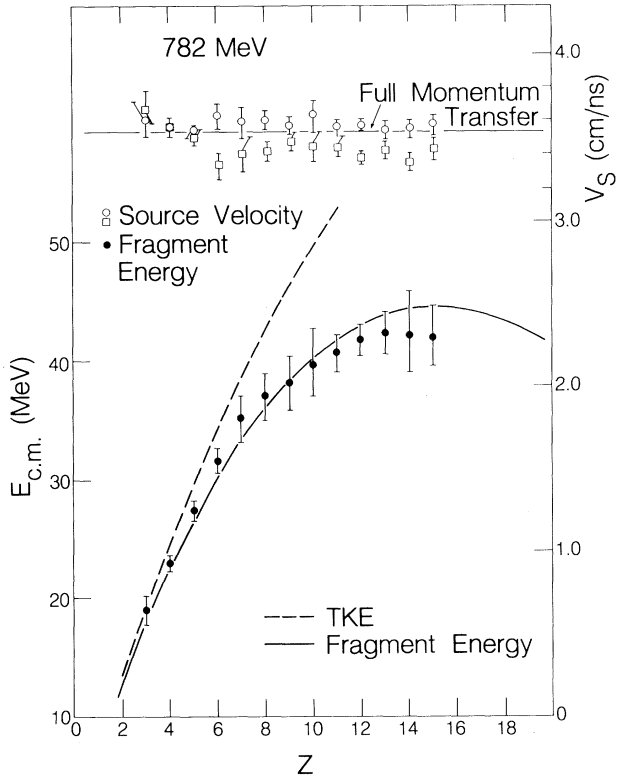

FIG. 3. The deduced c.m. energies (filled circles) and source velocities (open symbols) for the $^{93}Nb + ^{12}C$ system. Source velocities were determined with the assumption that the product mass followed the line of β stability (open circles) or the charge-equilibration line (open squares). A Coulomb calculation for two spheres is shown both for the c.m. energy of the light fragment (solid line) and the total kinetic energy (dashed line). The value of the source velocity expected for full momentum transfer is indicated by the horizontal line. The error bars indicate the uncertainty of the intersection point shown in Fig. 2.

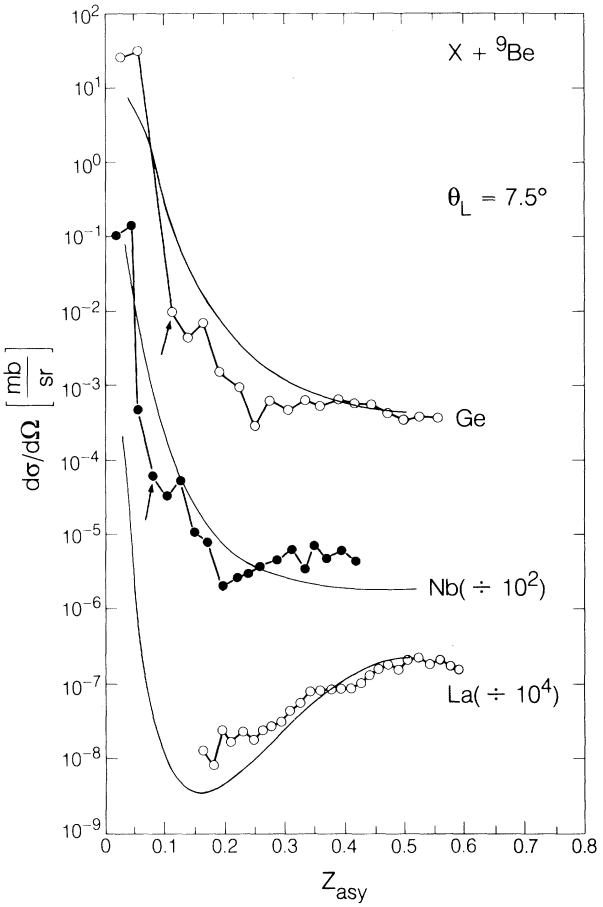

FIG. 4. Center-of-mass cross sections for products from the $^{74}Ge, ^{93}Nb, ^{139}La + ^9Be$ systems detected at $\theta_{lab} = 7.5°$. The solid line is a liquid-drop-model calculation of the fragment yield at $\theta_{c.m.} = 30°$. The arrows indicate the entrance-channel asymmetry. See text. Data below $Z_{asy} = 0.15$ were not obtained for the La + Be system, because of a limited dynamic range of the telescope.

tum transfer. For the other systems studied, the extracted source velocities are also independent of Z within a few percent of the velocity expected for full momentum transfer. The deduced c.m. energies are shown in the lower portion of Fig. 3. These energies are reproduced by a Coulomb calculation for two spheres with a surface separation of 2 fm. This same separation also reproduces the c.m. energies from the ^{74}Ge-induced reactions; however, a larger separation is required for the ^{139}La data. Both the full momentum transfer and the invariance with angle of the c.m. energies seen above are consistent with compound-nucleus decay.

The experimental cross sections for the systems 530-MeV ^{74}Ge, 782-MeV ^{93}Nb, and 1157-MeV ^{139}La on ^{9}Be are shown in Fig. 4. The cross sections are plotted as a function of charge asymmetry ($Z_{asy} = Z_{detected}/Z_{total}$). The lack of enhancement in yield near the target Z supports the compound-nucleus origin of the products rather than a deep-inelastic origin. The yield from the $^{74}Ge + ^9Be$ system, with a fissility parameter of $x = 0.31$, decreases steadily as one moves towards symmetry. The yields from the $^{93}Nb + ^9Be$ system ($x = 0.40$) are essentially constant from $Z_{asy} = 0.2$ to 0.4 while the yields from the $^{139}La + ^9Be$ system ($x = 0.50$) show the characteristic fission peak at symmetry. These three systems clearly exhibit the qualitative trends expected from the topological changes in the potential energy surface predicted by the liquid drop model[2,3] (see Fig. 1).

A quantitative comparison between these data

and a compound-nucleus calculation based upon the liquid drop model is also shown in Fig. 4. The absolute yields were calculated from the expression

$$\sigma_Z = \pi\lambda^2 \sum_{l=0}^{l_m} (2l+1) \frac{\Gamma_Z(l)}{\Gamma_n + \Gamma_p + \Gamma_\alpha}, \tag{1}$$

where

$$\frac{\Gamma_Z}{\Gamma_n} = \frac{T_z}{T_n} \left(\frac{E - B_n}{E - B_z} \right)^2 \exp\{2[a(E-B_z)]^{1/2} - 2[a(E-B_n)]^{1/2}\}$$

and l_m is the minimum of either $l_{\max}$ (the grazing angular momentum) or l_{crit} (the critical angular momentum for fusion[5]) and T_z is the temperature at the conditional saddle point. The expression for the decay width for each asymmetry was taken from Swiatecki[6] with the level-density parameter $a = A/8$. The barrier was taken to be

$$U = (U_3 + U_4 - U_{\text{CN}}) + U_{\text{C}} + U_{\text{prox}} + (U_{\text{rot}}^{\text{sp}} - U_{\text{rot}}^{\text{CN}}). \tag{2}$$

In this expression U_3, U_4, and U_{CN} are the droplet-model masses[7] of the exit-channel fragments 3 and 4 and the compound nucleus, respectively. The interfragment Coulomb energy (U_{C}) was calculated for spheres with a constant separation for each system chosen so that the center-of-mass energies reproduce the data (see Fig. 2). The nucleus-nucleus interaction is included via the proximity potential (U_{prox}). The l-wave dependence of the barrier height is included in the last two terms of Eq. (2), where the rotation energies of the compound nucleus and that of the dinuclear complex ($U_{\text{rot}}^{\text{SP}}$) (taken as two spheres with the appropriate separation) are taken into account. The mass for a given charge division was calculated (for $Z > 2$) from charge equilibration.

The angular distribution expressions given in Ref. 3 were employed to calculate the differential cross section ($d\sigma/d\Omega$). The c.m. angles of the data in Fig. 4 vary as a function of Z. However, the average c.m. angle is approximately 30°, and so this angle was chosen for comparison. The agreement in absolute magnitude and in trend between this calculation and the data confirms the compound-nuclear origin of these fragments.

In summary, we have shown that fragments with atomic numbers covering the entire range of the mass-asymmetry coordinate are produced from the decay of an excited compound nucleus. The observed Z distributions indicate that the topological transition expected at the Businaro-Gallone point does indeed take place in the region of $A \sim 100$. The exact position of the Businaro-Gallone point and its angular momentum dependence can in principle be established by a systematic study of the Z or A distributions as the fissility parameter x and the rotational parameter y are varied.

This work was supported by the Director, Office of Energy Research, Division of Nuclear Physics of the Office of High Energy and Nuclear Physics of the U. S. Department of Energy under Contract No. DE-AC03-76SF00098.

[a]Permanent address: Chemistry Department, Washington University, St. Louis, Mo. 63130.

[b]Permanent address: Centre d'Etudes Nucléaires de Saclay, F-91191 Gif-sur-Yvette Cedex, France.

[c]Permanent address: Shanghai Institute of Nuclear Research, Shanghai, China.

[d]Permanent address: Institute of Atomic Energy, Beijing, China.

[1]U. L. Businaro and S. Gallone, Nuovo Cimento **1**, 629, 1277 (1955).

[2]J. R. Nix, Nucl. Phys. **A130**, 241 (1969), and references therein.

[3]L. G. Moretto, Nucl. Phys. **A247**, 2111 (1975).

[4]L. G. Sobotka *et al.*, Phys. Rev. Lett. **51**, 2187 (1983).

[5]R. Bass, Nucl. Phys. **A231**, 45 (1974).

[6]W. J. Swiatecki, Lawrence Berkeley Laboratory Report No. LBL-11403 (unpublished).

[7]R. W. Hasse, Ann. Phys. (N.Y.) **68**, 377 (1971).